

NOTE

Impact of *Staphylococcus aureus* accessory gene regulator (*agr*) system on linezolid efficacy by profiling pharmacodynamics and RNAIII expression

Rachel L Soon¹, Justin R Lenhard¹, Irene Reilly¹, Tanya Brown¹, Alan Forrest¹ and Brian T Tsuji^{1,2}

The Journal of Antibiotics (2017) 70, 98–101; doi:10.1038/ja.2016.59; published online 8 June 2016

Clinical failures of vancomycin against methicillin-resistant *Staphylococcus aureus* (MRSA) have challenged its role as the therapeutic backbone for MRSA infections. The rise of strains with reduced vancomycin susceptibility,¹ together with low penetration rates to specific infection sites,^{2,3} and significant nephrotoxicity risks⁴ further contribute to concern regarding the utility of vancomycin.⁵ Consequently, newer anti-staphylococcal agents, such as linezolid, have drawn considerable attention as therapeutic alternatives. Linezolid exerts its mechanism of action by binding to the 23S ribosomal RNA of the *S. aureus* 50S subunit and interfering with the formation of the 70S initiation complex, thereby preventing translation of proteins.⁶ The relatively unique mechanism of action theoretically harbors little potential for cross-resistance with existing agents used to treat MRSA. In addition, linezolid exhibits potent activity against MRSA and superior pharmacokinetic properties in comparison to vancomycin^{7,8} with ~100% oral bioavailability and more extensive distribution at therapeutic concentrations.

Reduced vancomycin susceptibility in MRSA strains has been associated with a dysfunctional accessory gene regulator (*agr*) operon,^{9,10} which comprises four polymorphic groups (I–IV) that have a key role in regulating multiple virulence pathways through quorum sensing mechanisms. In comparison to strains with regular *agr* function, *S. aureus* strains dysfunctional in *agr* have been shown to require approximately fourfold-higher doses of vancomycin.¹⁰ In contrast, suppression of *agr* activity was recently demonstrated in the presence of clinically achievable concentrations of linezolid administered over 48 h.¹¹ Bacteriostasis was achieved against four MRSA strains (USA100, USA300, USA400 and ATCC 29213). Although these results are promising, the relationship between the *agr* operon and linezolid activity against *S. aureus* is unclear. Thus, the aim of the present study was to define the pharmacodynamics of linezolid against isogenic strains of *agr*-positive and *agr*-negative *S. aureus*. A secondary objective was to define the temporal association between linezolid exposure and *agr* function by profiling the primary transcript, RNAIII. *In vitro* time-kill and hollow-fiber models were

employed, with the latter designed to simulate human linezolid pharmacokinetics with clinical regimens.

Three *agr*-positive *S. aureus* strains harboring *agr*-groups I, II and IV (RN6390, RN6607 and RN4850, respectively), as well as isogenic strains negative for *agr*-groups I, II and IV (RN6911, RN9120 and RN9121, respectively) were obtained from the Network on Antimicrobial Resistance in *Staphylococcus aureus*. Prior to each experiment, solutions of linezolid were prepared from analytical grade powder (Pfizer, Groton, CT, USA) to achieve concentrations that ranged from $0.5 \times$ to $64 \times$ the MIC in twofold multiples (linezolid MIC = 1 mg l^{-1} for all strains, as determined by microdilution).¹² Cation-adjusted Mueller-Hinton broth (caMHB; Difco, Detroit, MI, USA; 12.5 mg l^{-1} magnesium and 25 mg l^{-1} calcium), and tryptic soy agar with 5% sheep's blood were utilized for all experiments. The inclusion of sheep's blood in tryptic soy agar plates allowed for the visualization of hemolysis by virulence factors under the control of the *agr* system and was used to confirm the absence or presence of *agr* activity. After achieving a starting inoculum of 10^6 CFU ml^{-1} , time-killing experiments were conducted over 48 h as described previously.¹³

In addition, a hollow-fiber infection model (HFIM) was used to investigate the *agr*-positive group II strain and the accompanying isogenic *agr*-negative group II strain as previously described.¹⁴ The *agr*-group II isolates were chosen for analysis in the HFIM because of previous suggestions that *agr* group II may be associated with resistance to other antimicrobials.⁹ Briefly, a cellulosic cartridge (FiberCell Systems, Frederick, MD, USA) incubating at 37°C was used to mimic a MRSA infection with a 10^6 CFU ml^{-1} bacterial load. Although bacteria were trapped in the extra-capillary space of the cartridge, fresh caMHB and linezolid were diffused through the porous fibers in a manner analogous to a circulatory system. Since the area under the concentration-time curve (AUC/MIC) is the pharmacokinetic index most predictive of linezolid efficacy, the linezolid infusion simulated the AUC achieved in the clinical regimen of 600 mg every 12 h ($f\text{AUC}_{0-24}$ 124), assuming a protein binding level of 31% and a terminal half-life of 4.8 h (fC_{max} 10.4 mg l^{-1}).¹⁵ At 0, 24,

¹Laboratory for Antimicrobial Pharmacodynamics, School of Pharmacy and Pharmaceutical Sciences, University at Buffalo, Buffalo, NY, USA and ²New York State Center of Excellence in Bioinformatics and Life Sciences, Buffalo, NY, USA

Correspondence: Dr BT Tsuji, Laboratory for Antimicrobial Pharmacodynamics, School of Pharmacy and Pharmaceutical Sciences, University at Buffalo, 701 Ellicott Street, Buffalo, NY 14203, USA.

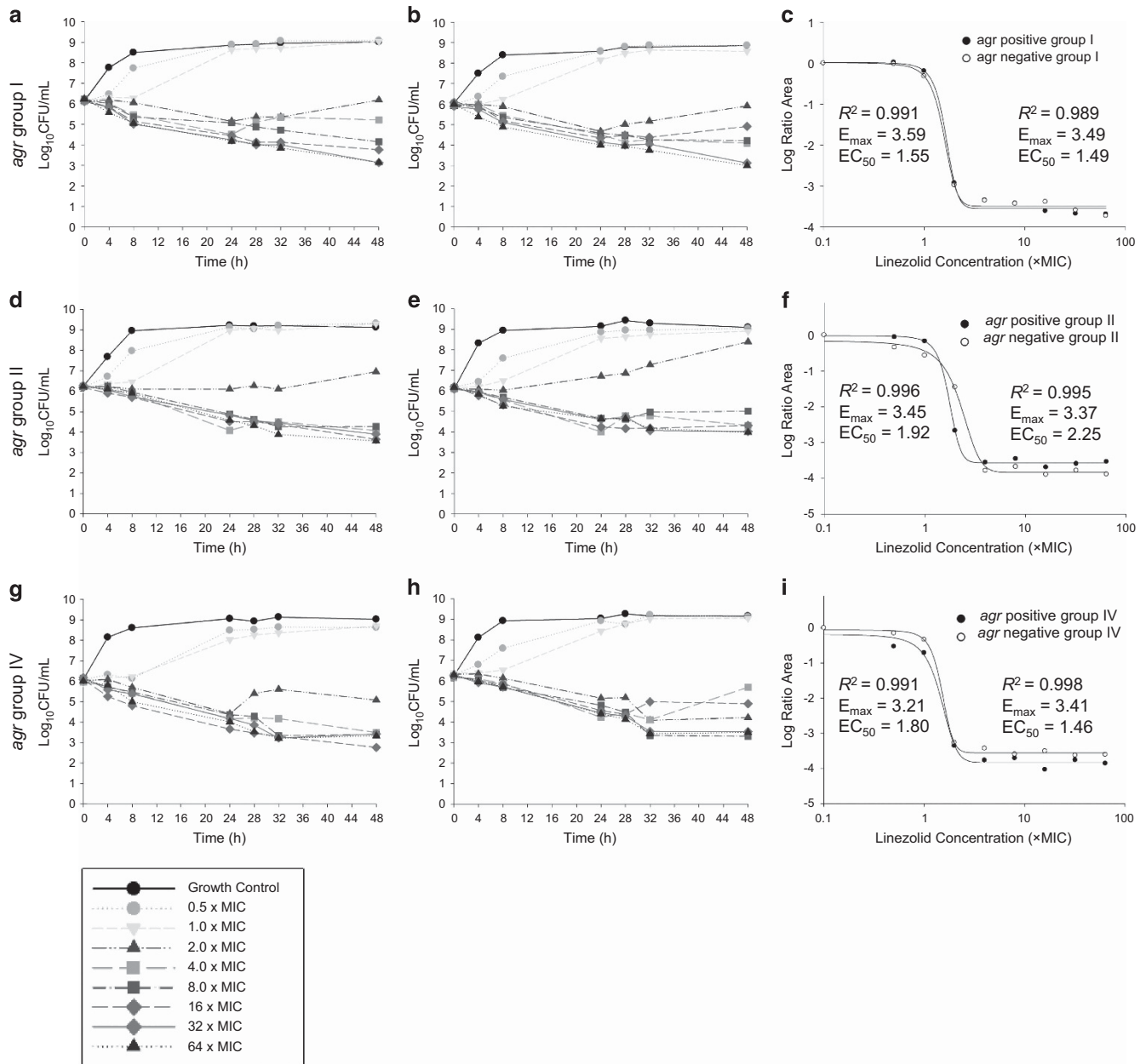
Email: btsuji@buffalo.edu

Received 1 February 2016; revised 16 April 2016; accepted 25 April 2016; published online 8 June 2016

48, 72, 96, 144, 192 and 240 h, samples were collected for viable bacterial counts, population analysis profiles, and RNAIII profiling (in the *agr*-positive strain). Population analysis profiles were conducted by plating bacterial samples onto Mueller-Hinton agar imbued with linezolid at 4, 8, and 16 mg l⁻¹. Samples were also centrifuged at 14 000 r.p.m. for 5 min then decanted; the supernatant was frozen at -80 °C and used for a quantitative real-time PCR analysis as detailed previously.¹¹

For time-killing experiments, an integrated pharmacokinetic-pharmacodynamic analysis was used to account for the entire

time-course of the experiments. For each linezolid concentration, the area under the CFU (AUCFU) curve was calculated and normalized by the AUCFU of the growth control. Taking the log of the normalized AUCFU yielded the log ratio area as shown in equation (1). Plotting the log ratio area for each linezolid concentration resulted in a sigmoidal curve that was fit with the Hill-type function in equation (2) (SYSTAT version 13.00.05, Systat Software Inc., Chicago, IL, USA). In equation (2), E_0 represents the bacterial killing effect of linezolid, E_{max} is the maximal drug effect, the EC_{50} is the concentration of



linezolid produces 50% of the maximal effect, C is the concentration of linezolid, and H is the sigmoidicity constant. Finally, an additional analysis was conducted in which the log ratio change ($\log_{10}\text{CFU ml}^{-1}$ reduction by 48 h) was calculated for each linezolid concentration and a paired t -test with two tails was used to assess differences between *agr*-positive and *agr*-negative strains (R Version 3.1.2).¹⁶

$$\text{Log ratio area} = \log_{10} \left(\frac{\text{AUCFU}_{\text{drug}}}{\text{AUCFU}_{\text{control}}} \right) \quad (1)$$

$$E = E_0 - \frac{E_{\text{max}} \times (C)^H}{(\text{EC}_{50})^H + (C)^H} \quad (2)$$

Time-killing profiles describing the effect of linezolid on the bacterial density ($\log_{10}\text{CFU ml}^{-1}$) of paired *agr*-positive (Figures 1a, d and g) versus-negative (Figures 1b, e and h) MRSA strains of *agr*-groups I, II and IV, are presented in Figure 1. In *S. aureus* strains containing *agr* groups I, II and IV, *agr* functionality did not alter the performance of linezolid. By 48 h, linezolid achieved a 3.10, 2.67 and 3.32 maximal $\log_{10}\text{CFU ml}^{-1}$ reduction (groups I, II and IV, respectively) against strains with a functional *agr* system, whereas the isogenic *agr* knockouts experienced a comparable 2.99, 2.19 and 2.93 maximal $\log_{10}\text{CFU ml}^{-1}$ reduction. Similarly, a paired t -test evaluating the log ratio change at 48 h for each linezolid concentration did not reveal a significant difference between *agr*-positive and *agr*-negative strains ($P=0.81, 0.07$ and 0.41 for *agr* groups I, II and IV, respectively).

To further evaluate how *agr* functionality impacts linezolid pharmacodynamics, a Hill-type function was used to integrate all the data obtained in CFU plots (Figure 1). Overall, the Hill-type function fit the data well with R^2 values exceeding 0.98 for each model. Parameter estimates from the Hill plots indicated that the maximal activity of linezolid was not altered by *agr* functionality: E_{max} values for *agr*-positive strains mirrored those of *agr*-negative strains (E_{max} *agr*-positive vs -negative = 3.59 vs 3.49, 3.45 vs 3.37, and 3.21 vs 3.41, *agr* groups I, II and IV, respectively). Moreover, differences in EC_{50} values for *agr*-positive and negative strains were $<0.35 \text{ mg l}^{-1}$ for all the *agr* groups investigated.

In addition to the time-killing experiments, a HFIM was used to simulate a linezolid regimen of 600 mg every 12 h against an *agr* group II positive strain and its accompanying isogenic *agr* knockout (Figure 2). After 240 h of linezolid exposure, 4.99 $\log_{10}\text{CFU ml}^{-1}$ ($\log_{10}\text{AUCFU} = 8.62 \log_{10}\text{CFU} \cdot \text{h ml}^{-1}$) of *agr*-positive *S. aureus* remained in the simulated infection site, whereas 4.41 $\log_{10}\text{CFU ml}^{-1}$ ($\log_{10}\text{AUCFU} = 8.03 \log_{10}\text{CFU} \cdot \text{h ml}^{-1}$) of the *agr* knockout

remained. Not only were the CFU plots similar between the *agr* functional strain and its accompanying *agr* knockout, but linezolid also completely suppressed the emergence of resistant subpopulations in both experiments. Furthermore, an RNAIII expression analysis of the *agr*-positive HFIM experiment found that RNAIII transcription transiently increased and plateaued between 24 and 72 h, followed by a general decrease in RNAIII expression that reached a nadir at 144 h (Figure 2, c). The transient increase in RNAIII transcription in the current study contrasts with a previous investigation that found RNAIII transcription continuously decreased in USA 300 during linezolid exposure.¹¹ However, the relative increase in RNAIII expression from baseline was relatively small ($<4 \times$ baseline) in the present investigation relative to the increase in RNAIII expression previously observed when USA 300 multiplied in the absence of linezolid exposure ($>10 \times$ baseline). Similarly, relative RNAIII expression also transiently increased $>10 \times$ baseline when USA 300 was exposed to 2 g of vancomycin q12h in a previous HFIM experiment.¹⁷

In the present study, we sought to characterize the impact of *agr*-dysfunction on linezolid pharmacodynamics. Time-killing studies evaluating *S. aureus* with a group I, II or IV *agr* system suggest *agr* dysfunction did not significantly alter the activity of linezolid. Although the attenuation of linezolid's activity approached significance for the *agr* group II knockout strain ($P=0.07$), an HFIM analysis demonstrated that *agr* group II dysfunction did not alter the performance of linezolid in a simulated 10 day infection. The HFIM also showed that administration of linezolid did not result in the emergence of resistant subpopulations regardless of *agr* functionality. However, the HFIM only profiled resistance over 10 days and utilized population analysis profiles with linezolid concentrations of 4, 8, and 16 mg l^{-1} . It is possible that prolonged exposure may result in the amplification of linezolid resistance that may not be detected by the 10 day population analysis profile analysis.

Determination of antimicrobial activity primarily entails consideration of the extent of bacterial killing achieved upon drug exposure; however, the antimicrobial influence on the expression of virulence factors which affect the pathogenesis of infection may also be integral in the overall assessment of efficacy. This is particularly true for *S. aureus*, which is notorious for producing a wide spectrum of toxins in a growth-dependent manner, coordinated through quorum sensing processes under the overall control of the *agr* regulatory locus.¹⁸ In the present investigation, the temporal RNAIII profile displayed in Figure 2c indicates that the reduction in RNAIII induced by traditional linezolid regimens against the *agr* group II strains was

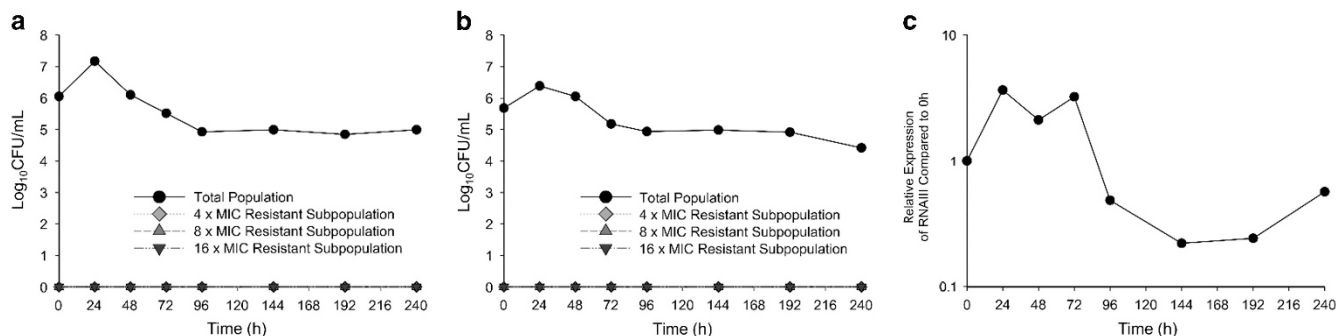


Figure 2 Hollow-fiber infection results illustrating the change in bacterial burden over 240 h for simulated linezolid regimens of 600 mg every 12 h against group II *agr*-positive (a) and *agr*-negative (b) *S. aureus*. The temporal profile of the primary transcript of *agr*, RNA III, by real-time PCR following exposure to the simulated linezolid regimens is also shown (c). A full color version of this figure is available at *The Journal of Antibiotics* journal online.

delayed, with a modest difference noted by 240 h in comparison with baseline. Linezolid may therefore help control virulence and play a pivotal role in severe toxin-mediated disease caused by certain MRSA strains.

Taken together, these data suggest that linezolid effectively overcomes *agr*-dysfunction and may play a primary role in toxin-mediated disease, offering a valuable therapeutic alternative for the treatment of MRSA strains resistant to vancomycin. Linezolid's ability to suppress the emergence of resistance and its favorable pharmacokinetic profile make the agent ideal in situations where vancomycin resistance is likely to develop due to low cell-wall penetrability, heterogeneous resistance, or for infections that entail a high bacterial density (for example, bilobar MRSA pneumonia). However, a significant limitation of the current study is the use of three out of four *agr* types, and it is possible that *agr* group III *S. aureus* strains may respond differently to linezolid exposure. Further *in vivo* investigations that quantify linezolid's impact on toxin release and the subsequent impact on immune-mediated bacterial clearance are needed to fully elucidate linezolid's utility in the treatment of MRSA infections.

CONFLICT OF INTEREST

The authors declare no conflict of interest.

- 1 Gomes, D. M., Ward, K. E. & LaPlante, K. L. Clinical implications of vancomycin heteroresistant and intermediately susceptible *Staphylococcus aureus*. *Pharmacotherapy* **35**, 424–432 (2015).
- 2 Graziani, A. L., Lawson, L. A., Gibson, G. A., Steinberg, M. A. & MacGregor, R. R. Vancomycin concentrations in infected and noninfected human bone. *Antimicrob. Agents Chemother.* **32**, 1320–1322 (1988).
- 3 Cruciani, M. *et al.* Penetration of vancomycin into human lung tissue. *J. Antimicrob. Chemother.* **38**, 865–869 (1996).
- 4 Wong-Beringer, A., Joo, J., Tse, E. & Beringer, P. Vancomycin-associated nephrotoxicity: a critical appraisal of risk with high-dose therapy. *Int. J. Antimicrob. Agents* **37**, 95–101 (2011).
- 5 Gould, I. M. Clinical activity of anti-Gram-positive agents against methicillin-resistant *Staphylococcus aureus*. *J. Antimicrob. Chemother* **66**, iv17–iv21 (2011).
- 6 Vardakas, K. Z., Ntziora, F. & Falagas, M. E. Linezolid: effectiveness and safety for approved and off-label indications. *Expert Opin. Pharmacother.* **8**, 2381–2400 (2007).
- 7 Wunderink, R. G. *et al.* Linezolid in methicillin-resistant *Staphylococcus aureus* nosocomial pneumonia: a randomized, controlled study. *Clin. Infect. Dis.* **54**, 621–629 (2012).
- 8 van Hal, S. J. & Paterson, D. L. New Gram-positive antibiotics: better than vancomycin? *Curr. Opin. Infect. Dis.* **24**, 515–520 (2011).
- 9 Sakoulas, G. *et al.* *Staphylococcus aureus* accessory gene regulator (*agr*) group II: is there a relationship to the development of intermediate-level glycopeptide resistance? *J. Infect. Dis.* **187**, 929–938 (2003).
- 10 Tsuji, B. T., Rybak, M. J., Lau, K. L. & Sakoulas, G. Evaluation of accessory gene regulator (*agr*) group and function in the proclivity towards vancomycin intermediate resistance in *Staphylococcus aureus*. *Antimicrob. Agents Chemother.* **51**, 1089–1091 (2007).
- 11 Tsuji, B. T. *et al.* Front-loaded linezolid regimens result in increased killing and suppression of the accessory gene regulator system of *Staphylococcus aureus*. *Antimicrob. Agents Chemother.* **56**, 3712–3719 (2012).
- 12 CLSI. Clinical Laboratory and Standards Institute (CLSI). Performance Standards for Antimicrobial Susceptibility Testing: 21st Informational Supplement. CLSI document M100-S21 (2011).
- 13 Tsuji, B. T., MacLean, R. D., Dresser, L. D., McGavin, M. J. & Simor, A. E. Impact of accessory gene regulator (*agr*) dysfunction on vancomycin pharmacodynamics among Canadian community and health-care associated methicillin-resistant *Staphylococcus aureus*. *Ann. Clin. Microbiol. Antimicrob.* **10**, 20 (2011).
- 14 Gumbo, T. *et al.* Selection of a moxifloxacin dose that suppresses drug resistance in *Mycobacterium tuberculosis*, by use of an *in vitro* pharmacodynamic infection model and mathematical modeling. *J. Infect. Dis.* **190**, 1642–1651 (2004).
- 15 Zvox Package Insert. New York, NY: Pfizer Inc, Revised 7/2015.
- 16 R Core Team. R: A Language and Environment for Statistical Computing. (R Foundation for Statistical Computing, Vienna, Austria, 2015).
- 17 Lenhard, J. R. *et al.* Sequential evolution of vancomycin-intermediate resistance alters virulence in *Staphylococcus aureus*: pharmacokinetic/pharmacodynamic targets for vancomycin exposure. *Antimicrob. Agents Chemother.* **60**, 1584–1591 (2015).
- 18 George, E. A. & Muir, T. W. Molecular mechanisms of *agr* quorum sensing in virulent staphylococci. *ChemBiochem.* **8**, 847–855 (2007).